Supplemental Data

Formation of a DTT-carbonate tetrahedral adduct in the active site of CocE: Complicating our structure determination efforts was exceptionally strong density in the active site that appeared to correspond to a covalent adduct with the catalytic serine of CocE (S117) (Fig. 7 and S1). Density was not previously reported (Larsen *et al.*, 2002). High quality electron density maps for this adduct corresponded to a five membered ring with two substituent arms. Anomalous difference Fourier maps confirmed the presence of sulfur in each of the arms, and $2F_o$-F_c omit maps contoured at different levels identified positions of atoms heavier than carbon, most likely oxygen, in the adduct (Fig. S1). The density was most consistent with a molecule of DTT, included at 1 mM concentration in the crystallization and harvesting solutions, that appears to have reacted with bicarbonate in the active site to form a 2-oxo-dioxolane ring, trapped as a tetrahedral intermediate dead-end complex, with one of the tetrahedral oxygen substituents occupying the oxyanion hole. In our highest resolution structure (L169K, Fig 7E & F), the carbon presumably donated by the carbonate in the dioxolane ring is ~1.6 Å from the S117 γ-oxygen (distance was not restrained in refinement of the high resolution structures), 1.5 Å from the oxygen in the oxyanion hole, and 1.4-1.5 Å from the two oxygen atoms donated by DTT. These distances are consistent with covalent bounds. The electron density of the tetrahedral carbon is weaker than that of the other carbons in the DTT ligand, suggesting electron withdrawal. The 2-oxo-dioxolane adduct adopts a similar conformation to the 2-phenylboronate adduct with CocE (Larsen *et al.*, 2002) .

To confirm that formation of this adduct complex was not a consequence of the stabilizing mutants, we determined the wt-CocE structure in the presence and absence of

DTT, and structures of stabilizing mutants of CocE were also determined in the absence of DTT (Fig S1, statistics reported on Supplemental Table 1). In all cases where DTT was co-crystallized with CocE, the adduct was observed, and the position of the H1-H2 loop was essentially the same with or without DTT. DTT was also tested for inhibition of CocE activity, but did not significantly affect CocE activity at concentrations of up to 3 mM [data not shown], and enzyme in the absence of DTT show similar thermal inactivation kinetics as those of enzymes in the presence of DTT. Crystals grown without DTT, or grown with DTT and subsequently soaked with atropine, a tropane analogue that is structurally similar to cocaine, appeared to displace the adduct (not shown). Instead, a water molecule binds near S117 and high B-factors are observed for active site residues, including S117 and H287 of the catalytic triad. No density was observed for atropine.

References

Larsen N.A., Turner J.M., Stevens J., Rosser S.J., Basran A., Lerner R.A., Bruce N.C. and Wilson I.A. (2002) *Nature structural biology,* **9**, 17-21. First published.

Figure S1

Comparison of DBC and Phenyl Boronic acid in the active site of wt-CocE. **A)** DBC was found covalently bound to the active site S117 of crystals grown from protein isolated with DTT. An omit map of the DBC molecule (left) shows carbon density at 5 sigma (light brown), oxygen density at 12 sigma (cyan), and sulfur density at 20 sigma (green**). B)** This panel depicts the previously reported binding site of the transition-state analog phenyl boronic acid (pdb:1JU3) (Larsen *et al.*, 2002), which is analogous to the DBC binding site. Omit map density for the L169K mutant is shown, which coordinates a water molecule which hydrogen bonds to the DBC ring.

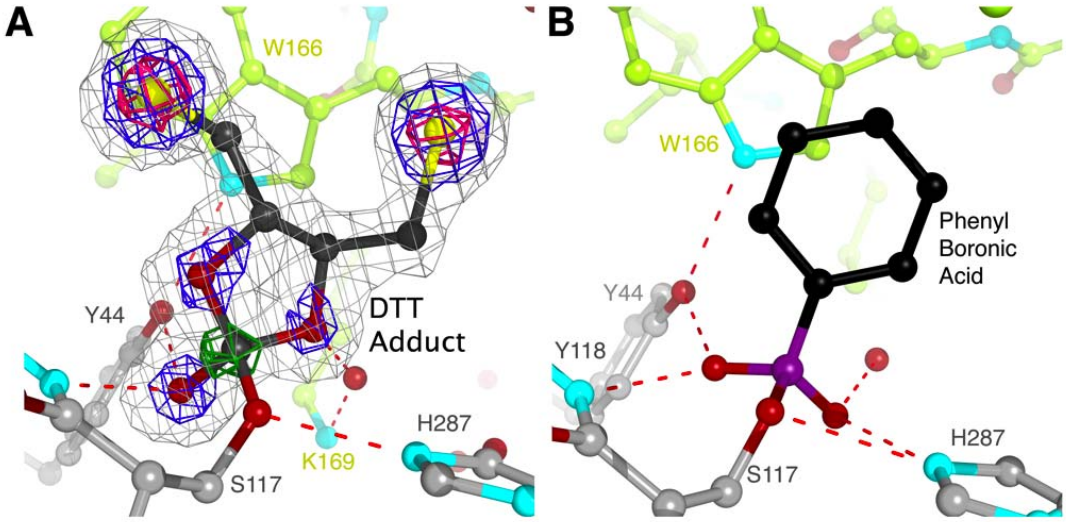
A
W166
Y44
DTT
Adduct
H287
K169
S117
B
W166
Phenyl
Boronic
Acid
Y44
Y118
H287
S117

Figure S1

Supplemental Table1.

Crystallographic data and refinement statistics

	WT no DTT	WT with DTT
X-ray Source:	APS 23-ID B	APS 21-ID D
Wavelength (Å)	1.033	1.000
Resolution (Å)	2.0	1.5
Space group	$p6_522$	$p6_522$
Cell constants (Å)	*a*=*b*=105.8, *c*=222.4	*a*=*b*=105.5, *c*=222.377
Unique reflections	50,037	114,702
Redundancy	10.8 (11.0)[a]	4.3 (3.0)[a]
R_{sym} (%)[b]	12.5 (58.6)	0.76 (54.4)
Completeness (%)	99.9 (100)	99.6 (100)
$\langle I \rangle / \langle \sigma_I \rangle$	31.6 (4.8)	35.1 (3.1)
Refinement statistics		
Resolution (Å)	20.0 – 2.01	20.0 – 1.51
Total reflections	47,307 (3,354)	108,618 (7,902)[c]
Protein atoms	4,827	4,884
Non-protein atoms	654	906
R.m.s.d. bond lengths (Å)	0.015	0.011
R.m.s.d. bond angles (°)	1.441	1.381
Est. coordinate error (Å)	0.078	0.054
Ramachandran plot		
most favored (%)	89.1	89.3
disallowed (%)	1.0	0.6
R_{work}[d]	14.1 (16.0)	13.0 (18.1)
R_{free}[e]	17.8 (23.1)	15.3 (22.1)

[a] Numbers in parentheses correspond to the highest resolution shell of data; data set WT no DTT: 2.07-2.00 Å; WT with DTT: 1.56-1.51 Å.

[b] $R_{sym} = \sum_{hkl}\sum_i |I(hkl)_i - I(hkl)|/ \sum hkl\ I(hkl)_i$, where I(*hkl*) is the mean intensity of *i* reflections after rejections. A –1.0 I/σ_I cutoff was applied to the T172R data set.

[c] Numbers in parentheses correspond to the highest resolution shell of data; WT no DTT: 2.06-2.01 Å; WT with DTT: 1.55-1.51 Å.

[d] $R_{work} = \sum_{hkl}||F_{obs}(hkl)| - |F_{calc}(hkl)||/ \sum_{hkl} |F_{obs}(hkl)|$; no I/σ cutoff was used during refinement.

[e] A portion (5%)of the truncated data set was excluded from refinement to calculate R_{free}.